Stable Single-Longitudinal-Mode Fiber Ring Laser Using Topological Insulator-Based Saturable Absorber

Shuqing Chen, Qingkai Wang, Chujun Zhao, Ying Li, Han Zhang, and Shuangchun Wen

***Abstract*—A single-longitudinal-mode (SLM) fiber ring laser based on topological insulator (TI) Bi_2Te_3 saturable absorber (SA) had been experimentally demonstrated. The TI: Bi_2Te_3 nanosheets, which were fabricated through the bottom-up approach, were coated onto the microfiber as an efficient saturable absorber device to ensure the SLM operation. Combined with fiber Bragg grating, the output wavelength can be continuously tuned about 1 nm. Without any accurate cavity control, stable SLM operation without mode hopping had been conveniently achieved. Based on the Lorentzian fitting, the line-width was measured to be less than 10 kHz. The output power of SLM fiber laser can reach up to 23 mW, indicating that the proposed TI-based SA may be suitable for high-optical power SLM operation in the future.**

***Index Terms*—Fiber laser, microfiber, single longitudinal mode, topological insulator.**

I. Introduction

SINGLE-longitudinal-mode (SLM) fiber lasers are of great interests due to their versatile applications in coherent communication, sensors, and microwave photonics [1]–[4]. In particular, erbium-doped fiber (EDF) lasers are very important because of the following merits: high output power, narrow line-width, and potentially all-fiber format [5]–[10]. Conventionally, most of them employed highly complex techniques, such as multiple ring cavity structures [11], tunable ring resonators [12], and external light injection [13]–[17]. Simple configurations have also been demonstrated by using un-pumped EDFs as saturable absorber [18]–[22]. However, due to high insertion losses, more extra pump power is needed. And the direct method to improve the output power is to increase the pump power, but the excessive input power limits further improvement of output power due to the extra burden which general apparatus suffered, especially for saturable absorber based SLM operation [23]. Commonly, the general SLM fiber lasers have a lower scalable output power less than 10 mW, especially for material-based saturable absorber SLM fiber laser [24], [25]. So searching for a method with simple and high optical power tolerance structure to generate SLM operation is extremely significant.

Recently, graphene has been attaining rising attentions in both photonics and optoelectronics applications due to its unique electronic band structure and optical properties [26]–[28]. Numerous contributions have reported that graphene can show plenty of optical applications, such as broadband saturable absorber for mode-locked fiber laser [29], [30], stable four wave mixing (FWM) effect induced multi-wavelength laser [31], and SLM lasers [24], [25]. However, graphene has relatively low damage threshold and low saturable intensity [32]. Especially, saturable absorber with sandwiched structures is easier to suffer high power density, which may lead to saturable absorber is more vulnerable to damage. And the SLM operation by using such graphene-SA is not easy to achieve moderate optical power (e.g., 10 mW) [24], [25]. Very recently, topological insulator, a kind of Dirac materials characterized by metallic surface state in association with bulk insulating state [33], [34], was found to show saturable absorption at telecommunication wavelength [35], 800 nm [36], 1064 nm [37], and 1645 nm [38], respectively. Zhang *et al*. also found that TI shows giant nonlinear refractive index of 10^{-14} m^2/W [36]. Unlike graphene, saturable absorption in TI originates from the Pauli-blocking principle of the electrons filled either in the metallic surface state or in the bulk insulating state [35]. This means that TI possesses two different types of saturable absorption mechanisms, each of which can contribute the light-matter interaction. Those results caught our attention on whether the TI can be developed as SA in SLM operation? The microfiber based SA, such as TI/graphene covered tapered fiber [39], has widely applied in the pulse laser generation due to its advantage of high optical power handling [40].

In this contribution, a novel, simple and short cavity design of SLM EDF laser by using a TI-based saturable absorber was experimentally demonstrated. In the cavity, a tapered fiber based TI fabricated by the optical deposition method was embedded as SA. And a FBG was used to select specific signal wavelength in order to stabilize the single wavelength operation. By which, the interferogram were formed by the input and feedback light. Depending on the saturable absorption effect, the weaker mode can be effectively suppressed, and the stronger mode is very

Manuscript received June 17, 2014; revised September 14, 2014, August 15, 2014, and August 10, 2014; accepted September 14, 2014. Date of publication September 16, 2014; date of current version October 15, 2014. This work was supported by the National 973 Program of China under Grant 2012CB315701, the National Natural Science Foundation of China under Grant 61025024 and 61205091, and Hunan Provincial Natural Science Foundation of China under Grant 12JJ7005. *(Corresponding authors: H. Zhang and Y. Li.)*

S. Chen, C. Zhao, Y. Li, and H. Zhang are with the SZU-NUS Collaborative Innovation Center for Optoelectronic Science and Technology, and Key Laboratory of Optoelectronic Devices and Systems of Ministry of Education and Guangdong Province, Shenzhen University, Shenzhen 518060, China (e-mail: shuqingchen@yeah.net; chujunzhao@gmail.com; queenly@vip.sina.com; hzhang@szu.edu.cn).

Q. Wang and S. Wen are with the Key Laboratory for Micro-/Nano- Optoelectronic Devices of Ministry of Education, College of Physics and Microelectronic Science, Hunan University, Changsha 410082, China (e-mail: 79792239@163.com; scwen@vip.sina.com).

Color versions of one or more of the figures in this paper are available online at http://ieeexplore.ieee.org.

Digital Object Identifier 10.1109/JLT.2014.2358855

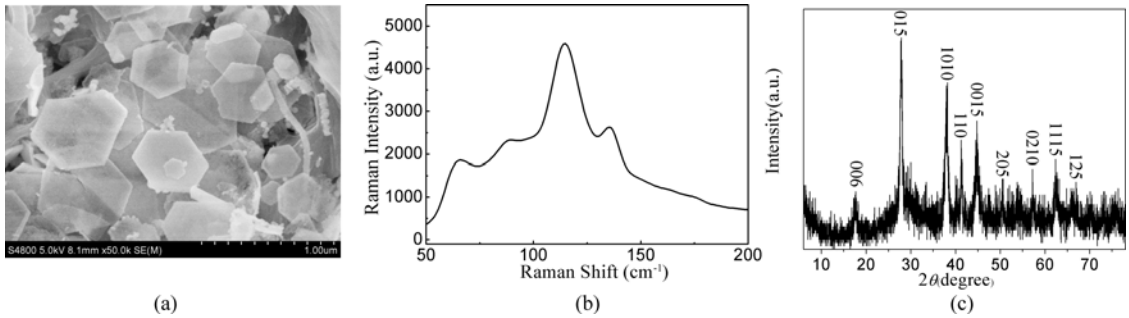

Fig. 1. (a) Scanning electron microscopy (SEM), and (b) Raman spectra (c) the XRD pattern of Bi_2Te_3 nanosheets.

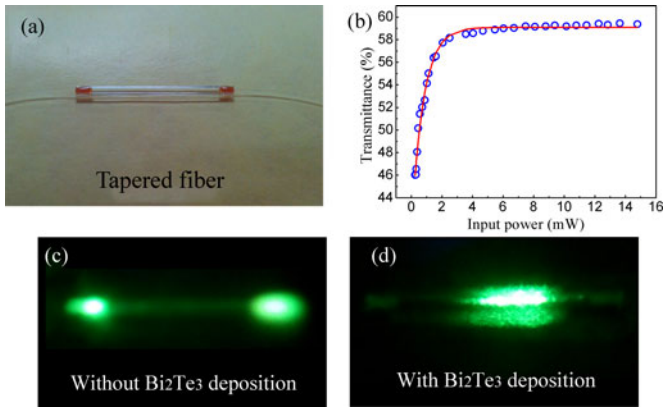

Fig. 2. (a) The image of the tapered fiber, and optical microscopy images of a tapered fiber without (b), with (c) TI deposition obtained by Infrared Viewer, and (d) the measured saturable absorption data and its corresponding fitting curve.

few are absorbed by the saturable absorber. This effectively ensured the realization of SLM operation. Because of the light interaction with TI was implemented by evanescent wave, the proposed SAs were more suitable for high optical power operation. As the optical source with power of ~1 W was injected, SLM operation with output power as high as 23 mW had been obtained. By mechanical stressing FBG, output wavelength can be tuned from 1542.3 nm to 1543.2 nm. With the employment of 1 Gb/s OOK (On Off Keying) signal, RF beating signal at 1 GHz had been generated by using optical heterodyne technique. Upon fitting the electrical spectrum of the beating signal by Lorentzian function, the SLM line-width was measured to be less than 10 kHz.

II. Design and Fabrication of Microfiber-Based TI Saturable Absorber

The operation principle of the TI: Bi_2Te_3 deposited tapered fiber is based on the interaction of TI: Bi_2Te_3 nanosheets with evanescent field of the propagating light in the fiber. The TI: Bi_2Te_3 nanosheets were synthesized by diethylene glycol (DEG) mediated polyol method. In typical synthesis, a stoichiometric ratio of bismuth nitrate ($Bi(NO_3)$), and potassium telluride (K_2TeO_3) were dissolved in DEG with vigorous stirring followed by refluxing the mixture solution at 240 °C for 4–5 h. Then, the mixture was cooled down to room temperature. The gray powders were collected by filtering, washed with distilled water and ethanol, and finally dried at 60 °C in vacuum overnight. The as-grown and washed powders were dispersed in an ethanol solution.

Fig. 1 shows the representative scanning electron microscopy (SEM) image and Raman spectra of Bi_2Te_3 nanosheets. As in Fig. 1(a), the field-emission scanning electron microscopy (FE-SEM) shows that a large number of randomly dispersed sheet-like structures had been successfully fabricated. The prepared nanosheets are predominantly hexagonal-based sheets with uniform size and well-defined shape. The edge length is in the range of 400–500 nm. And the Bi_2Te_3 nanosheets were characterized by Raman spectrum. Raman spectroscopy, which is a sensitive probe to the local atomic arrangements and vibrations of the materials, has been widely used to investigate the microstructure of the nano-sized materials. As shown in Fig. 1(b), three Brillion zone centers Raman active modes at A_{1g}^1, E_g^2 and A_{1g}^2 are observed, which are located at 65.5, 88.7 and 134.2 cm^{-1}, respectively. Besides, an additional peak with obvious intensity at ~114 cm^{-1} is identified as A_{1u} mode composed of longitudinal optical phonons at the Brillion zone boundary. The strongest A_{1u} peak is due to the crystal symmetry breaking of nanoplatelets with thin thickness. And the XRD (X-ray diffraction) pattern of the freshly prepared products is shown in Fig. 1(c). All the diffraction peaks can be indexed to rhombohedral Bi_2Te_3 (space group: $R\bar{3}m$) with lattice constants $a = b = 0.438$ nm, $c = 3.048$ nm (JCPDS No. 15-0863). This result indicates that Bi_2Te_3 products obtained via our synthetic method consist of a pure phase.

As shown in Fig. 2, a piece of tapered fiber with stretching length of 24 mm and diameter of about 13 μm was under our investigation. The insertion loss of this tapered fiber is lower than 0.5 dB. And the tapered fiber was encapsulated in a half round glass tube, as shown in Fig. 2(a). In the following, light with wavelength at 975 nm was launched into the sample, and TI: Bi_2Te_3 solution was introduced into glass tube for optical deposition. The power of the injected light was about 100 mW. After 50 min, TI: Bi_2Te_3 nanosheets were deposited on the tapered fiber. In the following, we directed light into the tapered fiber with ~100 mW/975 nm to observe the change of the tapered fiber before and after the deposition of TI: Bi_2Te_3 nanosheets

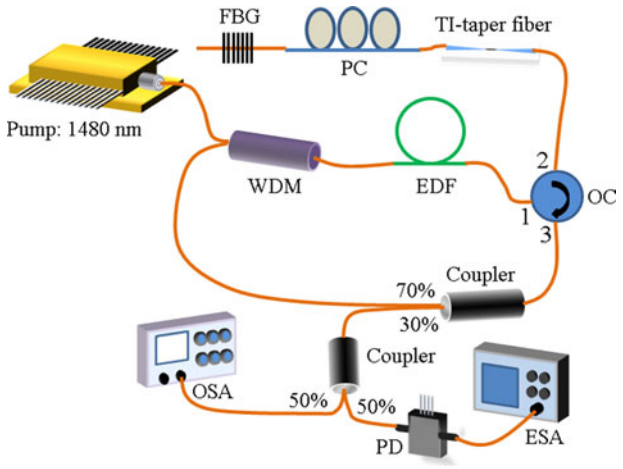

Fig. 3. Experimental setup of TI-based longitudinal mode laser, FBG: fiber Bragg grating, PC: polarization controller, OC: optical circulator, WDM: wavelength-division multiplexer, PD: photoelectric detector, TI-taper fiber: TI-deposited taper fiber.

by infrared viewer, as shown in Fig. 2(b) and (c). Without the deposition, scattering occurred at the both ends of the glass tube induced by encapsulation. After the deposition, obviously, light was heavily scattered at the central part of the tapered fiber, which was caused by the leakage of the evanescent field due to the existence of high refractive index materials like TI: Bi_2Te_3 nanosheets. This phenomenon is clearly shown in Fig. 2(c), which indicates the good deposition of TI: Bi_2Te_3 nanosheets. And the balanced twin-detector measurement was employed to characterize the nonlinear optical response of the TI-SA. The transmittance as a function of the incident laser power at 1542 nm (pico-second fiber laser, repetition rate: 6.025 MHz, pulse width: 1.8 ps) was shown in Fig. 2(d). By fitting the curve, the optical modulation depth is inferred to be about 18%.

III. Experiment and Results

Fig. 3 shows the experimental setup of the proposed SLM fiber ring laser. The total cavity length is about 12 m, and a piece of 1 m highly-doped erbium-doped fiber (EDF, LIEKKI Er 80-8/125) with group velocity dispersion of –20 ps^2/km was used as the gain medium. The EDF was pumped by a laser diode source of wavelength 1480 nm, a 1480/1550 wavelength-division multiplexer (WDM) was used to couple the pump light into the cavity, and the EDF was then connected to the port 1 of an optical circulator (OC). In between the port 2 of OC and the FBG, a tapered fiber coated with TI: Bi_2Te_3 was introduced to operate as the saturable absorber to generate the SLM operation. And FBG serves as a coarse wavelength selector with the reflection peak at 1542.3 nm. Port 3 of the OC was connected to a 70:30 fiber coupler with the 70% port connecting back to the 1550 nm port of the WDM, and the 30% port was employed for the output of the signal. And a polarization controller (PC) was employed to control the polarization state of the light.

Fig. 4(a) shows the output optical spectrum of SLM operation. The wavelength of the output is about 1542.3 nm and the side-mode suppression ratio of this laser line is larger than 40 dB. By carefully adjusting the PC under a pump power of 1W, we had obtained the stable single longitudinal mode operation. The output power could be continuously increased up to about 23 mW. The repeated scans of the lasing lines at 10-min interval over 3 h at room temperature are shown in Fig. 4(b). As shown in Fig. 5, the wavelength variation is kept nearly constant while the maximum output power fluctuation is lower than 1 dB, indicating the good stability of the SLM system.

By applying mechanical stress upon the FBG, the wavelength tuning range of the ring fiber laser spanning from 1542.3 to 1543.2 nm had been obtained. The tuning range is limited due to the design of the FBG, and it can be further enhanced by properly designing the FBG [18]. Fig. 6 shows the output spectra versus wavelength tuning while the other conditions were kept constant. We could clearly note that the optical spectra showed good stability within the entire tuning range.

Fig. 7 shows the variation of the peak amplitude power against the tuned SLM wavelength. The obtained distribution of SNR is between 46.9 and 47.5 dB. And there is an insignificant output power variation over the entire range of wavelengths, and the peak power fluctuation is kept lower than 1 dB.

The SLM operation could be further verified through monitoring the beating signals of the longitudinal modes at a 5 GHz photo-detector cascaded with a 7 GHz electrical spectral analyzer. Without incorporating the saturable absorber, the electrical frequency spectrum of the beating signal from 0 to 1 GHz is shown in Fig. 8(a). It was found that a number of beating signals of the laser longitudinal modes had been observed which can be ascribed to the laser longitudinal mode beating, and the mode-spacing is about 17.4 MHz. The appearance of multiple beating signals indicate that the fiber laser operates in multiple longitudinal oscillations. However, once the saturable absorber device is introduced into the laser cavity, multiple beating signals could suddenly disappear from the electrical spectrum of beating signal shown in Fig. 8(b). As seen from the figure, no beating signal frequencies to the round-trip frequency of the fiber ring laser and its multiples were monitored, indicating that the laser now operated in SLM. The repeated scans of the electrical spectrum of beating signal at 10-min interval over an hour at room temperature were also recorded. As shown in Fig. 9(a), there is no apparent mode-hopping effects were discovered, which also means that the laser operates in the SLM regime all the time. And when we tuning the FBG, the corresponding electrical spectrum were also recorded. As shown in Fig. 9(b), with the wavelength tuned from 1542.37 to 1543.16 nm, the SLM operation is kept all the range. Which all verified that the laser can well worked in the SLM operation.

We have exploited the optical heterodyne technique to verify the SLM operation of the proposed EDF laser, and measured the spectral line width. The delayed self-heterodyne method was employed with a 10 km fiber delay line and an intensity modulator. The modulator was driven by the 1 Gb/s OOK signal, and the corresponding heterodyne radio frequency (RF) spectrum is demonstrated in Fig. 10. As shown in Fig. 10(a), the RF beating signal at 1 GHz was generated, and with span of 1 GHz, there is not any other longitudinal mode beating observed, further

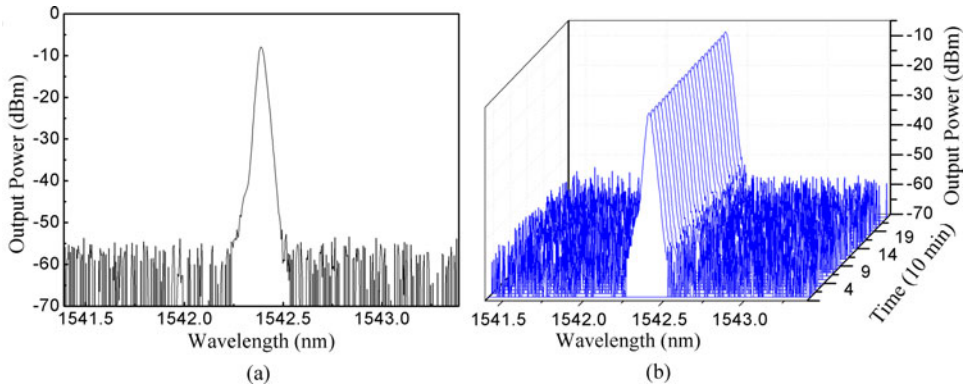

Fig. 4. (a) The output spectrum of single longitudinal mode operation, and (b) the corresponding spectra taken at a 10-min interval over 3 h.

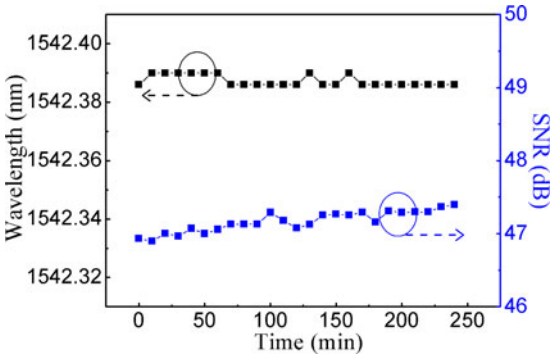

Fig. 5. Wavelength variation and output power fluctuation with scanning over 3 h.

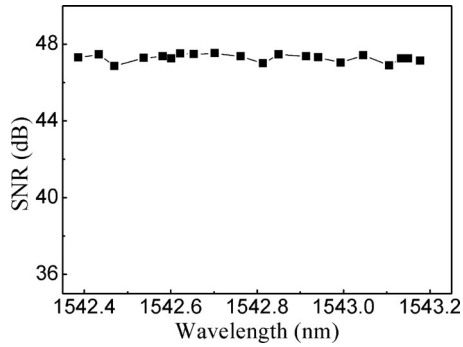

Fig. 7. SNR versus wavelengths in the tuning range of 1542.3–1543.2 nm.

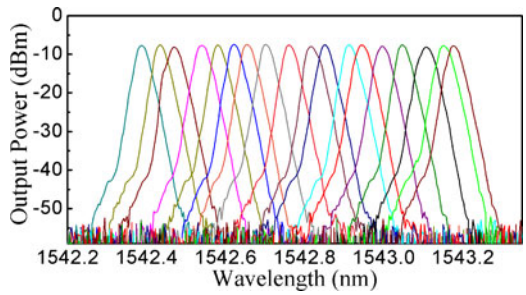

Fig. 6. Output spectra versus wavelength in the tuning range of 1542.3–1543.2 nm.

indicating that the laser operates in the SLM regime. With a frequency span of 1 MHz, the zoom-in view of the beat signal is shown in Fig. 10(b), in which we take 3 dB down from the maximum value and observe that 3 dB bandwidth is less than 10 kHz, which can be confirmed by the Lorentzian fitting.

We also conduct another experiment, where we employed a FBG with central wavelength at about 1570.1 nm to select the wavelength. The repeated scans of the output optical spectrum of the proposed laser at 10-min interval over 2 h at room temperature were recorded, which shows in Fig. 11(a). As shown in Fig. 11(b), the maximum output power fluctuation is also lower than 1dB, indicating that the proposed laser possess good stability of the output at L-band. As we applied mechanical stress upon the FBG, the wavelength of the ring fiber laser was tuned from 1570.182 to 1571.012 nm. Its output spectra were shown in Fig. 12(a) and (b). And the corresponding electrical spectrum of the beating signal was shown in Fig. 12(c) and (d). As shown in Fig. 12(c) and (d), there are no apparent mode-hopping effects were discovered, which indicate that the laser can efficiently ensure the SLM operation at 1570 nm (L-band). This result clearly shows that our topological insulator saturable absorber could allow for the generation of SLM operation at the L-band.

IV. Conclusion

High-power SLM operation (with output power up to 23 mW) at telecommunication band had been successfully demonstrated in an EDF ring laser enabled by topological insulator materials. This saturable absorber device was directly fabricated through the optical deposition method and then integrated with the tapered micro-fiber, which can guarantee the beneficial effect of light interaction with topological insulator, and also possess the advantages of being able to alleviate thermal loading and enduring high power illumination. The fiber laser consists of a piece of FBG in order to initiate the single wavelength emission. Based on the optical heterodyne technique, the measured line-width is measured to be less than 10 kHz, clearly indicating the SLM operation. Our contributions evidence that topological insulator

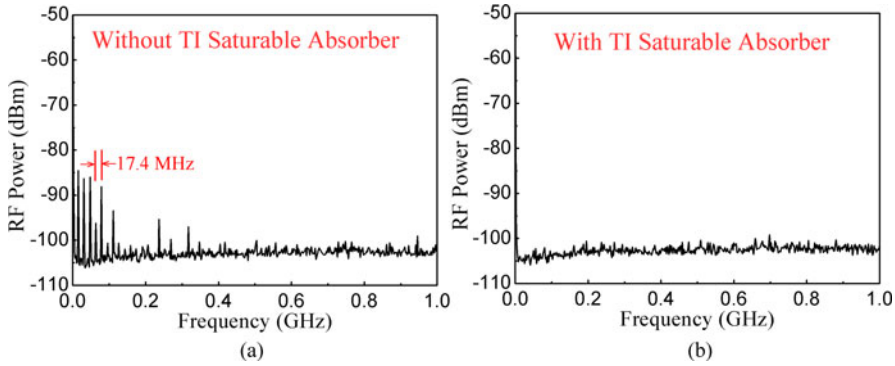

Fig. 8. Electrical spectrum of the beating signal, (a) without saturable absorber, and (b) with saturable absorber incorporated in the laser cavity.

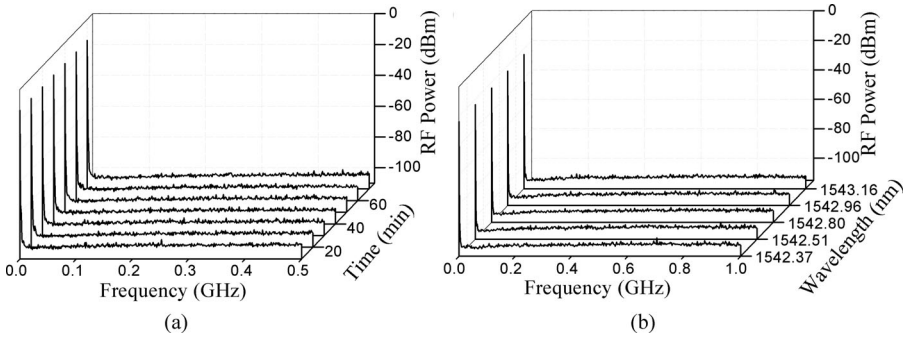

Fig. 9. Electrical spectrum of SLM operation; (a) taken at a 10-min interval over 1 h and (b) as the FBG tuning.

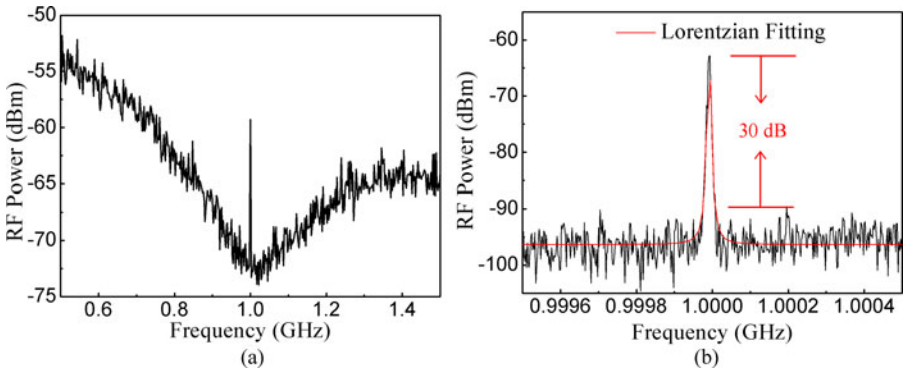

Fig. 10. Delay self-heterodyne RF beating spectrum; (a) 2 GHz span with resolution of 30 kHz and (b) 1 MHz span with resolution of 500 Hz.

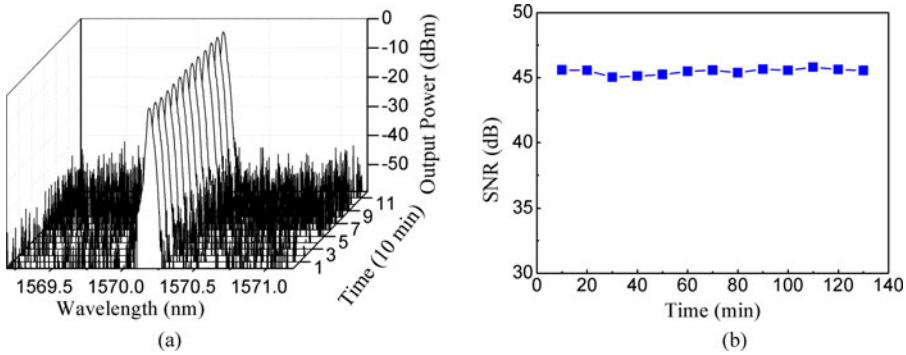

Fig. 11. (a) The repeated scans of the output optical spectrum of the proposed laser at 10-min interval over 2 h, (b) output power fluctuation with scanning over 2 h.

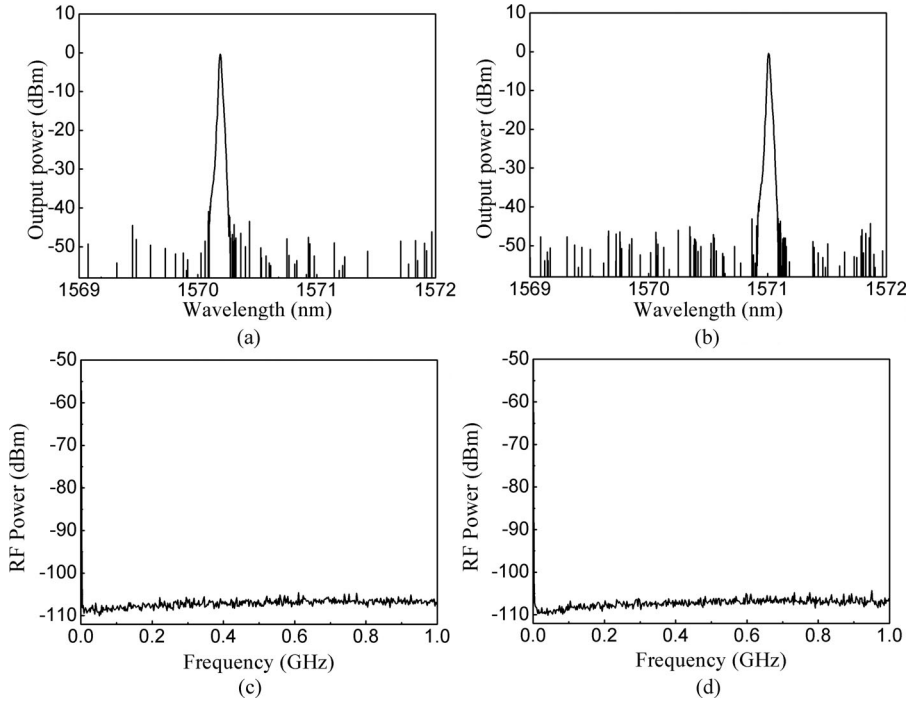

Fig. 12. Output spectra versus wavelength in the 1570.182 nm (a) and 1571.012 nm (b), respectively. And (c), (d) are the corresponding electrical spectrum of the beating signal.

materials may be developed as an efficient saturable absorber suitable for the generation of high-power and broadband SLM and may find applications for SLM (from C-band to L-band) related microwave photonics.

REFERENCES

[1] S. Pan and J. A. Yao, "A wavelength-switchable single-longitudinal-mode dual-wavelength erbium-doped fiber laser for switchable microwave generation," *Opt. Exp.*, vol. 17, no. 7, pp. 5414–5419, Mar. 2009.

[2] X. P. Cheng, P. Shum, C. H. Tse, J. L. Zhou, M. Tang, R. F. Wu, and J. Zhang, "Single-longitudinal-mode erbium-doped fiber ring laser based on high finesse fiber Bragg grating Fabry–Pérot etalon," *IEEE Photon. Technol. Lett.*, vol. 20, no. 12, pp. 976–978, Jun. 2008.

[3] N. Libatique, L. Wang, and R. Jain, "Single-longitudinal-mode tunable WDM-channel-selectable fiber laser," *Opt. Exp.*, vol. 10, no. 25, pp. 1503–1507, Dec. 2002.

[4] X. Y. He, X. Fang, C. L. Liao, D. N. Wang, and J. Q. Sun, "A tunable and switchable single-longitudinal-mode dual-wavelength fiber laser with a simple linear cavity," *Opt. Exp.*, vol. 17, no. 24, pp. 21773–21781, Nov. 2009.

[5] X. Chen, Z. Deng, and J. Yao, "Photonic generation of microwave signal using a dual-wavelength single-longitudinal-mode fiber ring laser," *IEEE Trans. Microw. Theory.*, vol. 54, no. 2, pp. 804–809, Feb. 2006.

[6] J. L. Zhou, L. Xia, X. P. Cheng, X. P. Dong, and P. Shum, "Photonic generation of tunable microwave signals by beating a dual-wavelength single longitudinal mode fiber ring laser," *Appl. Phys. B*, vol. 91, no. 1, pp. 99–103, Apr. 2008.

[7] J. Capmany and D. Novak, "Microwave photonics combines two worlds," *Nature Photon.*, vol. 1, no. 6, pp. 319–330, Jun. 2007.

[8] B. Lin, S. C. Tjin, H. Zhang, D. Y. Tang, S. Liang, J. Z. Hao, and B. Dong, "Dual-wavelength single-longitudinal-mode erbium-doped fiber laser based on inverse-gaussian apodized fiber bragg grating and its application in microwave generation," *Opt. Fiber Technol.*, vol. 17, no. 2, pp. 120–123, Mar. 2011.

[9] J. Zhang, C. Y. Yue, G. G. Schinn, W. R. L. Clements, and W. Y. John, "Stable single-mode compound-ring erbium-doped fiber laser," *J. Lightw. Technol.*, vol. 14, no. 1, pp. 104–109, Jan. 1996.

[10] W. S. Liu, M. Jiang, D. Chen, and S. L He, "Dual-wavelength single-longitudinal-mode polarization-maintaining fiber laser and its application in microwave generation," *J. Lightw. Technol.*, vol. 27, no. 20, pp. 4455–4459, Oct. 2009.

[11] C. H. Yeh, T. T. Huang, H. C. Chien, C. H. Ko, and S. Chi, "Tunable S-band erbium-doped triple-ring laser with single-longitudinal-mode operation," *Opt. Exp.*, vol. 15, no. 2, pp. 382–386, Jan. 2007.

[12] P. L. Scrivener, E. J. Tarbox, and P. D. Maton, "Narrow linewidth tunable operation of Er^{3+} -doped single-mode fibre laser," *Electron. Lett.*, vol. 25, no. 8, pp. 549–550, Apr. 1989.

[13] X. Zhang, N. H. Zhu, L. Xie, and B. X. Feng, "A stabilized and tunable single-frequency erbium-doped fiber ring laser employing external injection locking," *J. Lightw. Technol.*, vol. 25, no. 4, pp. 1027–1033, Apr. 2007.

[14] C. C. Lee and S. Chi, "Single-longitudinal-mode operation of a grating-based fiber-ring laser using self-injection feedback," *Opt. lett.*, vol. 25, no. 24, pp. 1774–1776, Dec. 2000.

[15] V. V. Spirin, C. A. L. Mercado, P. Mégret, and A. A. Fotialdi, "Single-mode Brillouin fiber laser passively stabilized at resonance frequency with self-injection locked pump laser," *Laser Phys. Lett.*, vol. 9, no. 5, pp. 377–380, Mar. 2012.

[16] W. T. Tsang and R. A. Logan, "Observation of enhanced single longitudinal mode operation in 1.5-μm GaInAsP erbium-doped semiconductor injection lasers," *Appl. Phys. Lett.*, vol. 49, no. 25, pp. 1686–1688, Oct. 1986.

[17] M. Yamada and Y. Suematsu, "A condition of single longitudinal mode operation in injection lasers with index-guiding structure," *IEEE J. Quantum Electron.*, vol. 15, no. 8, pp. 743–749, Aug. 1979.

[18] H. Ahmad, M. Z. Zulkifli, A. A. Latif, M. H. Jemangin, S. S. Chong, and S. W. Harun, "Tunable single longitudinal mode S-band fiber laser using a 3 m length of erbium-doped fiber," *J. Mod. Opt.*, vol. 59, no. 3, pp. 268–273, Feb. 2012.

[19] R. K. Kim, S. Chu, and Y. G. Han, "Stable and widely tunable single-longitudinal-mode dual-wavelength erbium-doped fiber laser for optical beat frequency generation," *IEEE Photon. Technol. Lett.*, vol. 24, no. 6, pp. 521–523, Mar. 2012.

[20] X. He, D. N. Wang, and C. R. Liao, "Tunable and switchable dual-wavelength single-longitudinal-mode erbium-doped fiber lasers," *J. Lightw. Technol.*, vol. 29, no. 6, pp. 842–849, Mar. 2011.

[21] W. S. Liu, M. Jiang, D. Chen, and S. L He, "Dual-wavelength single-longitudinal-mode polarization-maintaining fiber laser and its application in microwave generation," *J. Lightw. Technol.*, vol. 27, no. 20, pp. 4455–4459, Oct. 2009.

[22] Y. Yao, X. Chen, Y. Dai, and S. Z. Xie, "Dual-wavelength erbium-doped fiber laser with a simple linear cavity and its application in microwave generation," *IEEE Photon. Technol. Lett.*, vol. 18, no. 1, pp. 187–189, Jan. 2006.

[23] X. X. Yang, L. Zhan, Q. S. Shen, and Y. X. Xia, "High-power single-longitudinal-mode fiber laser with a ring fabry–perot resonator and a saturable absorber," *IEEE Photon. Technol. Lett.*, vol. 20, no. 11, pp. 879–881, Jun. 2008.

[24] H. Ahmad, M. Z. Zulkifli, A. A. Latif, and S. W. Harun, "Tunable radio frequency generation using a graphene-based single longitudinal mode fiber laser," *J. Lightw. Technol.*, vol. 30, no. 13, pp. 2097–2102, Jul. 2012.

[25] F. D. Muhammad, M. Z. Zulkifli, A. A. Latif, S. W. Harun, and H. Ahmad "Graphene-based saturable absorber for single-longitudinal-mode operation of highly doped erbium-doped fiber laser," *IEEE Photon. J.*, vol. 4, no. 2, pp. 467–475, Apr. 2012.

[26] Q. Bao and K. P. Loh, "Graphene photonics, plasmonics, and broadband optoelectronic devices," *ACS Nano*, vol. 6, no. 5, pp. 3677–3694, May. 2012.

[27] K. S. A. Novoselov, A. K. Geim, S. V. Morozov, D. Jiang, M. I. Katsnelson, I. V. Grigorieva, S. V. Dubonos, and A. A. Firsov, "Two-dimensional gas of massless dirac fermions in graphene," *Nature*, vol. 438, no. 7065, pp. 197–200, Jul. 2005.

[28] A. K. Geim and K. S. Novoselov, "The rise of graphene," *Nature Mater.*, vol. 6, no. 3, pp. 183–191, Mar. 2007.

[29] Z. Sun, T. Hasan, F. Torrisi, D. Popa, G. Privitera, F. Q. Wang, F. Bonaccorso, D. M. Basko, and A. C. Ferrari, "Graphene mode-locked ultrafast laser," *Acs Nano*, vol. 4, no. 2, pp. 803–810, Jan. 2010.

[30] H. Zhang, D. Tang, R. J. Knize, L. M. Zhao, Q. L. Bao, and K. P. Loh, "Graphene mode locked, wavelength-tunable, dissipative soliton fiber laser," *Appl. Phys. Lett.*, vol. 96, no. 11, pp. 111112-1–111112-3, Mar. 2010.

[31] H. Ahmad, A. A. Latif, M. I. M. A. Khudus, A. Z. Zulkifli, M. Z. Zulkifli, K. Thambiratna, and S. W. Harun, "Highly stable graphene-assisted tunable dual-wavelength erbium-doped fiber laser," *Appl. Opt.*, vol. 52, no. 4, pp. 818–823, Feb. 2013.

[32] Z. W. Zheng, C. J. Zhao, S. B. Lu, Y. Chen, Y. Li, H. Zhang, and S. C. Wen, "Microwave and optical saturable absorption in graphene," *Opt. Exp.*, vol. 20, no. 21, pp. 23201–23214, Oct. 2012.

[33] H. J. Zhang, C. X. Liu, X. L. Qi, X. Dai, Z. Fang, and S. C. Zhang, "Topological insulators in Bi_2Se_3, Bi_2Te_3 and Sb_2Te_3 with a single dirac cone on the surface," *Nature Phys.*, vol. 5, no. 6, pp. 438–442, May. 2009.

[34] J. E. Moore, "The birth of topological insulators," *Nature*, vol. 464, no. 7286, pp. 194–198, Mar. 2010.

[35] S. Q. Chen, C. J. Zhao, Y. Li, H. H. Huang, S. B. Lu, H. Zhang, and S. C. Wen, "Broadband optical and microwave nonlinear response in topological insulator," *Opt. Mater. Exp.*, vol. 4, no. 4, pp. 587–596, Apr. 2014.

[36] S. B. Lu, C. J. Zhao, Y. H. Zou, S. Q. Chen, Y. Chen, Y. Li, H. Zhang, S. C. Wen, and D. Y. Tang, "Third order nonlinear optical property of Bi_2Se_3," *Opt. Exp.*, vol. 21, no. 2, pp. 2072–2082, Jan. 2013.

[37] Z. Q. Luo, Y. Z. Huang, J. Weng, H. H. Cheng, Z. Q. Lin, B. Xu, Z. P. Cai, and H. Y. Xu, "1.06 μm Q-switched ytterbium-doped fiber laser using few-layer topological insulator Bi_2Se_3 as a saturable absorber," *Opt. Exp.*, vol. 21, no. 24, pp. 29516–29522, Dec. 2013.

[38] P. H. Tang, X. Q. Zhang, C. J. Zhao, Y. Wang, H. Zhang, D. Y. Yuang, S. C. Wen, D. Y. Tang, and D. Y. Fan, "Topological insulator: Bi_2Te_3 saturable absorber for the passive Q-switching operation of an in-band pumped 1645-nm Er: YAG ceramic laser," *IEEE Photon. J.*, vol. 5, no. 2, pp. 1500707–1500707, Apr. 2013.

[39] J. Z. Wang, Z. Q. Luo, M. Zhou, C. C. Ye, H. Y. Fu, Z. P. Cai, H. H. Cheng, H. Y. Xu, and W. Qi, "Evanescent-light deposition of graphene onto tapered fibers for passive Q-switch and mode-locker," *IEEE Photon. J.*, vol. 4, no. 5, pp. 1295–1305, Oct. 2012.

[40] C. Liu, C. C. Ye, Z. Q. Luo, H. H. Cheng, D. D. Wu, Y. L. Zheng, Z. Liu, and B. Qu, "High-energy passively Q-switched 2 μm Tm^{3+} -doped double-clad fiber laser using graphene-oxide-deposited fiber taper," *Opt. Exp.*, vol. 21, no. 1, pp. 204–209, Jan. 2013.

Authors' biographies not available at the time of publication.